

<https://helda.helsinki.fi>

Genetic and Epigenetic Characterization of Growth Hormone-Secreting Pituitary Tumors

Välimäki, Niko

2019-12

Välimäki , N , Schalin-Jäntti , C , Karppinen , A , Paetau , A , Kivipelto , L , Aaltonen , L A &
Karhu , A 2019 , ' Genetic and Epigenetic Characterization of Growth Hormone-Secreting
Pituitary Tumors ' , Molecular Cancer Research , vol. 17 , no. 12 , pp. 2432-2443 . <https://doi.org/10.1158/1541-7786>

<http://hdl.handle.net/10138/323526>

<https://doi.org/10.1158/1541-7786.MCR-19-0434>

acceptedVersion

Downloaded from Helda, University of Helsinki institutional repository.

This is an electronic reprint of the original article.

This reprint may differ from the original in pagination and typographic detail.

Please cite the original version.

1 **Genetic and epigenetic characterization of growth hormone - secreting pituitary**
2 **tumors**

3 Niko Välimäki,^{1,2} Camilla Schalin-Jääntti,³ Atte Karppinen,⁴ Anders Paetau,⁵ Leena Kivipelto,⁴ Lauri A
4 Aaltonen,^{1,2} Auli Karhu^{1,2*}

5 ¹Department of Medical and Clinical Genetics, University of Helsinki, 00014 Helsinki, Finland

6 ²Applied Tumor Genomics, Research Programs Unit, FI-00014 University of Helsinki, Finland

7 ³Endocrinology, Abdominal Center, University of Helsinki and Helsinki University Hospital, 00029 Helsinki,
8 Finland

9 ⁴Department of Neurosurgery, University of Helsinki and Helsinki University Hospital, 00029 Helsinki,
10 Finland

11 ⁵Department of Pathology, HUSLAB, University of Helsinki, 00014 Helsinki, Finland

12
13 **Running title:** Genetic and epigenetic characterization of somatotropinomas

14 **Key words:** Pituitary tumor, Somatic landscape, Aneuploidy, DNA methylation, Tumor subtypes

15 **Financial support:** This work was supported by grants from the Academy of Finland's Center of Excellence
16 Program 2012–2017 (#250345) and 2018–2025 (#31204) (LAA, AK), the Academy of Finland (#287665)
17 (NV), and the Finnish Cancer Society (160081) (AK), the Helsinki University Hospital Research Funds
18 (TYH2017138 and TYH2018223) (CSJ) and Finska Läkaresällskapet (CSJ).

19 **Corresponding author:** Auli Karhu, Biomedicum Helsinki, Research Programs Unit, PO Box 63
20 (Haartmaninkatu 8), 00014 University of Helsinki, Tel: +358 2 94125612, E-mail: auli.karhu@helsinki.fi

21 **Conflict of Interest Disclosure:** The authors declare no potential conflicts of interest

22

23 Abstract

24 Somatic driver mechanisms of pituitary adenoma pathogenesis have remained incompletely characterized and
25 apart from mutations in the stimulatory $G\alpha$ protein ($G\alpha_s$ encoded by *GNAS*) resulting activated cAMP
26 synthesis, pathogenic variants are rarely found in growth hormone-secreting pituitary tumors
27 (somatotropinomas).

28 The purpose of the current work was to clarify how genetic and epigenetic alterations contribute to the
29 development of somatotropinomas by conducting an integrated copy-number alteration, whole-genome- and
30 bisulfite sequencing, and transcriptome analysis of 21 tumors. Somatic mutation burden was low but
31 somatotropinomas formed two subtypes associated with distinct aneuploidy rates and unique transcription
32 profiles. Tumors with recurrent chromosome aneuploidy (CA) were *GNAS* mutation negative (*Gsp*⁻). The
33 chromosome stable (CS) –group contained *Gsp*⁺ somatotropinomas and two totally aneuploidy-free *Gsp*⁻
34 tumors. Genes related to the mitotic G1/S-checkpoint transition, were differentially expressed in CA- and CS-
35 tumors indicating difference in mitotic progression. Also pituitary tumor transforming gene 1 (PTTG1), a
36 regulator of sister chromatid segregation, showed abundant expression in CA-tumors. Moreover,
37 somatotropinomas displayed distinct *Gsp* genotype-specific methylation profiles. Expression quantitative
38 methylation (eQTM) analysis revealed that inhibitory $G\alpha$ ($G\alpha_i$) –signaling is activated in *Gsp*⁺ tumors.

39 These findings suggest that in *Gsp*⁻ somatotropinomas aneuploidy through modulated driver pathways may be
40 a causative mechanism for tumorigenesis, whereas *Gsp*⁺ tumors in response to mitogenic cAMP-signaling
41 caused by *GNAS* mutation are characterized by DNA methylation activated $G\alpha_i$ –signaling.

42 **Significance:** These findings provide valuable new information about subtype-specific pituitary tumorigenesis
43 and may help to elucidate the mechanisms of aneuploidy also in other tumor types.

44

45 **Introduction**

46 Pituitary adenomas are common and comprise 15% of all diagnosed intracranial neoplasms. The overall rate
47 of pituitary tumors in the general population is one case in 1064 [1]. The most common functioning pituitary
48 tumors hypersecrete prolactin (PRL) (40%). Growth hormone (GH) –secreting adenomas (somatotropinomas)
49 constitute 15-20%, and usually lead to increased height (gigantism) in children or adolescents. In adults,
50 hypersecretion of GH causes acromegaly, and leads to overgrowth of bone and cartilage, insulin resistance,
51 hypertension, cardiovascular and respiratory complications, and increased risk of neoplasms. Despite being
52 benign, excess GH production is associated with increased morbidity and reduced life expectancy [2, 3, 4].

53 The majority of pituitary adenomas arise in a sporadic setting and are considered to be unicellular in origin.
54 As in other neoplasms, pituitary tumor formation and dysregulated hormone secretion are results of series of
55 genetic and epigenetic alterations upsetting the balance between proliferation and apoptosis. The most
56 frequently described somatic pathogenic events occurring in somatotropinomas are gain-of-function mutations
57 in the *stimulatory guanine nucleotide (GTP) binding protein alpha* ($G\alpha_s$) encoded by the *GNAS* gene. This
58 *Gsp* oncogene contributes to constitutive synthesis of cyclic adenosine monophosphate (cAMP), activation of
59 protein kinase A (PKA) pathway, and subsequent tumor formation. *Gsp* mutations occur in ~35% of
60 somatotropinomas [5, 6]. Next generation sequencing has shown that the somatic background of pituitary
61 adenomas is calm and single nucleotide- (SNV) and structural variants (SV) are rarely found. Therefore, the
62 exact mechanisms of tumorigenesis often remain unknown [7, 8, 9, 10, 11, 12].

63 Numerical alterations of whole chromosomes, aneuploidy, is observed in a subset of pituitary tumors [8, 12].
64 Aneuploidy is frequently noted in solid and malignant tumors and is often associated with tumor recurrence
65 and drug resistance in some tumor types [13, 14]. Shuffling of genomic content through aneuploidy facilitates
66 loss of heterozygosity (LOH) of tumor suppressors and increases copy number of oncogenes and can constitute
67 a powerful driver for tumor progression. In addition, epigenetic modifications associated to changes in gene
68 expression are considered potential causes of pituitary tumor initiation and development [15].

69 Apart from the *Gsp*⁺ driver mutation, mechanisms of pituitary adenoma pathogenesis have remained
70 incompletely characterized, and improved understanding of uncontrolled cell growth associated with pituitary
71 tumors is required. The purpose of the current work was to clarify how somatic alterations drive development
72 of somatotropinomas and discover subgroup-specific somatic patterns. This was done by dissecting

73 associations between somatic copy number alterations (SCNA), gene expression and DNA methylation in
74 *GNAS* mutation negative (*Gsp*⁻) and positive (*Gsp*⁺) pituitary tumors. In addition, whole genome sequencing
75 (WGS) was performed to identify somatic SNV and SV changes.

76 Here we found that somatotropinomas form two tumor subtypes associated with distinct aneuploidy rates and
77 transcription profiles. Our results indicate that defective chromosomal segregation may underlie the
78 development of aneuploidy and tumor initiation in a subset of *Gsp*⁻ somatotropinomas. Further, we show that
79 *Gsp* mutation status is the major determinant of methylation profiles of somatotropinomas, and that
80 methylation regulated transcription activates an adaptive response to elevated cAMP levels in *Gsp*⁺ tumors.

81 **Material and Methods**

82 **Patient material**

83 We studied somatotropinomas from twenty one patients (13 males and 8 females, mean age at diagnosis 43
84 years [range 14-69 years]) (Table 1). The tumor samples were collected between 2009 and 2015 at the Helsinki
85 University Hospital and frozen while fresh. The study was approved by the Ethics Committee of the Hospital
86 district of Helsinki (Dnr. 408/13/03/03/2009). All patients had given informed consent for sample collection
87 and analysis. In the case of minor, a parent gave the consent. All research conformed with the principles of the
88 Declaration of Helsinki. The tumor percentages (>95%) were verified with hematoxylin and eosin stainings.
89 All patients were mutation negative for the established germline mutations associated with pituitary neoplasia
90 (Supplementary Methods). Seven tumors were *Gsp*⁺ and 14 tumors *Gsp*⁻. Seven patients have hormonally
91 active disease and are treated with post-operative somatostatin analogue therapy (ST3, ST6, ST13, ST16,
92 ST17, ST19, ST21), one (ST6) of them is on somatostatin-cabergoline combination therapy and two (ST3,
93 ST17) on somatostatin-pegvisomant combination therapy. Currently, 14 patients are in hormonal remission,
94 while three non-compliant patients (ST3, ST7, ST22) are not, and current medical therapy of four patients
95 (ST2, ST8, ST14, ST15) is not known (Table 1).

96 **WGS, SCNA and gene expression profiling**

97 Genomic DNA was extracted by FastDNA Spin Kit (MP Biomedicals) (tumors) and DNeasy Blood and Tissue
98 Kit (Qiagen) (blood). The *AIP* and *Gsp* mutation status was identified by capillary sequencing as described
99 earlier [6]. The WGS genomic DNA libraries were prepared according to Illumina PE sequencing protocols

100 and sequenced to at least 40x median coverage on the Illumina HiSeq 2000 platform (2x100bp PE) (Beijing
101 Genomics Institute, BGI Tech Solutions Co., Ltd., China). A genome-wide analysis of tumors for somatic
102 SNVs and SVs was performed as described previously [8]. The somatic variants in tumors ST2-12 were
103 identified by filtering against a patient-matched blood sample. For the *Gsp*- tumors ST13, ST16, ST18-ST20
104 and ST22, patient-matched germline variants were not available, and somatic variants were identified by
105 filtering against all variants in gnomAD (r2.0.1) (<https://gnomad.broadinstitute.org>), 1000 genomes project
106 (phase 3, 20130502) (<http://www.internationalgenome.org/home>), Sequencing Initiative Suomi (SISu,
107 accessed on March 2016) (<http://www.sisuproject.fi/>) and an in-house collection of 339 normal tissue WGS
108 samples. The remaining variants were filtered to a minimum coverage of 10 reads, minimum alternative allele
109 coverage of six, and minimum quality score of 40 (phred-scale).

110 SCNA analysis was performed using SNP arrays (1kGP HumanOmni2.5-8 BeadChip, Illumina, Inc.). Analysis
111 was performed as described previously [8] comparing individuals' tumor sample to its corresponding normal
112 blood derived DNA using Genomics Suite v.6.5 (Partek) with a GC-wave correction. Genomic instability
113 percentage (GI%) was determined by dividing the number of altered chromosomal arms in the tumor by the
114 total number of chromosomal arms.

115 RNA was extracted with RNeasy Mini Kit (Qiagen). Expression profiles were generated using GeneChip™
116 Human Transcriptome Array 2.0 array (Thermo Fisher Scientific). cDNA synthesis, labeling, and
117 hybridization was performed according to the manufacturer's instructions. Quality control, normalization, and
118 analysis of data were carried out using Transcriptome Analysis Console v 3.0 (Thermo Fisher Scientific).
119 Unsupervised hierarchical clustering of 1000 probes with the largest variance was done using cosine distance
120 with bottom-up average linking. The annotation file HTA-2_0.na35.2.hg19.transcript and ANOVA were used
121 to determine differentially expressed genes between tumor groups. Differentially expressed genes were filtered
122 using false discovery rate (FDR)< 5% and fold change |FC| > 2.

123 **Bisulfite sequencing and data processing**

124 The target region bisulfite sequencing (TBS) of somatotropinomas was performed utilizing the SureSelectXT
125 Human Methyl. Seq (Agilent Technologies, Inc.) target enrichment system. Illumina paired-end sequencing
126 for libraries was done using 126 base-pair read length and the HiSeq2500 platform (Illumina, Inc.) (Beijing
127 Genomics Institute, BGI Tech Solutions Co., Ltd.).

128 The raw TBS data were preprocessed with the bismark (v0.16.3) pipeline, bowtie2 (v2.3.0) and the human
 129 reference genome (UCSC hg19). A total of 8,493,667 CpGs were observed with a minimum coverage of two,
 130 out of which 4,527,285 CpGs passed the minimum coverage in at least four tumors. CpG methylation levels
 131 were quantified using bsseq (v1.10.0) and DSS (v2.14.0) as follows. An unsupervised, genome-wide analysis
 132 was done using bsseq quantification of the CpG methylation levels: the TBS target regions (N=350,539) were
 133 filtered to a minimum of three CpGs that passed minimum coverage (N=198,649). The default bsseq
 134 smoothing was applied to quantify the methylation level of each target region. An unsupervised hierarchical
 135 clustering of 50 000 TBS regions with the largest variance was done using cosine distance with bottom-up
 136 average linking. Supervised analysis of differentially methylated regions (DMRs) used the default DSS
 137 smoothing to test for a minimum mean methylation difference of 0.2 in a two-group comparison. The DMRs
 138 were filtered with the default DSS settings (a minimum of 3 CpGs, minimum 50 bps and $P < 10^{-5}$).
 139 The gene annotation and their genomic coordinates were based on Ensemble (v82, hg19). The promoter regions
 140 were defined as going from -1kb to +2kb relative to the transcription starting site (TSS), gene bodies (+2kb,
 141 relative to the TSS, to the end of the gene). Other genomic annotations were downloaded from the UCSC table
 142 browser (accessed on August 2017) for ENCODE enhancer regions (6 human cell lines; awg segmentation
 143 combined), DNaseI Hypersensitivity Clusters (ENCODE v3), ENCODE transcription factor clusters (TFBS
 144 clusters v3; 161 factors) including the CCCTC-binding factor (CTCF) sites, and CpG islands [16]. CpG island
 145 shores were composed of 2kb upstream and downstream regions flanking the CpG islands. Methylation
 146 differences with regards to replication timing were annotated based on HeLa cell line data [17].
 147 CpG methylation levels were quantified within [0, 1], where 0 and 1 correspond to total absence and presence
 148 of the mark respectively.

149 **Expression quantitative methylation (eQTM) analysis**

150 eQTM analysis was used to identify association between methylation and gene expression levels. The DMRs
 151 and their nearby genes were tested for association, also known as cis-eQTM [18], using MatrixEQTL (v2.1.1).
 152 The cis-eQTMs were filtered to a maximum 20 Kbp distance between the gene and DMR. The resulting
 153 associations were filtered to FDR < 5%.

154 **Pathway analyses**

155 The pathway data was generated with Ingenuity Pathways Analyses (IPA) software
156 (<https://www.qiagenbioinformatics.com/products/ingenuity-pathway-analysis>. IPA Summer 2018 Release).
157 The data was mapped into relevant pathways based on their functional annotation and known molecular
158 interactions in Ingenuity's Knowledge Base (IPKB). The -log of p-value were calculated by Fisher's exact test.
159 A data set derived from expression arrays along with the corresponding FC and FDR p-values was uploaded
160 into IPA. The eQTM data set was mapped into relevant pathways in a similar manner.

161 **Immunohistochemistry (IHC)**

162 KI-67 (MIB-1) and PTTG1 (pituitary tumor transformation gene 1) IHCs were performed as described earlier
163 [8]. Other antibodies used were protein tyrosine phosphatase, receptor type D (PTPRD) rabbit Anti-PTPRD
164 (HPA054829, 1:300) (Sigma-Aldrich), protein tyrosine phosphatase, receptor type K (PTPRK) rabbit Anti-
165 PTPRK (HPA054822, 1:400) (Sigma-Aldrich), retinoblastoma (RB1) rabbit Anti-RB1 (HPA050082, 1:500)
166 (Sigma-Aldrich) and anti-Rb (phosphor-S780) (ab47763, 1:70) (Abcam). Anti-mouse/rabbit/rat secondary
167 antibody, Poly-HRP-GAM/R/R (DPVB55HRP, Immunologic) and DAB chromogen (Thermo Fisher
168 Scientific) were used for detection. Ki-67 and PTTG1 scores were obtained by calculating the average
169 percentage of stained cells among the tumor cell population. PTPRD, PTPRK and RB1 proteins were scored
170 by evaluating fractions of immunopositive cells and staining intensities. For scoring details see the
171 Supplementary Methods.

172 **Availability of data and materials**

173 Data has been deposited at the European Genome-phenome Archive (EGA) hosted by the EBI and the CRG,
174 under accession number EGAS00001003488.

175 **RESULTS**

176 **Somatic SNV and indel background of *Gsp*- somatotropinomas**

177 The somatic landscape of the tumors ST2-ST12 was reported previously [8]. The tumors had an average of 2.3
178 coding region SNVs per tumor, with *GNAS* being the only recurrently mutated gene. Here we examined the
179 somatic SNVs and SVs of six additional *Gsp*- tumors: ST13, ST16, ST18-20, and ST22. Supplementary Table
180 S1 gives all the coding region (missense, premature stop codon, frameshift) variants that passed the somatic
181 filtering. These additional *Gsp*- tumors had an excess of somatic variants - in total 92 coding region SNVs and
182 on average 15.3 SNVs per tumor – simply because rare germline variants may have passed the population-

183 based filtering. The majority of the somatic variants (47 SNVs) arise from ST22 due to patient's Italian
184 ancestry being underrepresented among the population-based controls. Among the 21 tumors studied the only
185 recurrently mutated gene was *GNAS*. No focal deletions or complex chromosomal rearrangements were
186 observed with exception of ST3, a previously reported *Gsp*⁺ tumor [8] (Supplementary Fig. S1).

187 **SCNA and expression profiling differences in CA- and CS -tumors**

188 Data from 21 somatotropinoma normal/tumor pairs was used for SCNA analysis. Results of eleven
189 normal/tumor pairs were from our earlier work [8]. Analyses revealed that 12 *Gsp*⁻ tumors contained frequent
190 and recurrent (≥ 4 tumors share the event) chromosomal deletions (chr 1, 4, 6, 14, 15, 16, 18, 22). Also gains
191 (chr 5, 7, 9, 19, 20) of entire chromosomes were detected, although with considerably lower frequency
192 (Supplementary Fig. S1). Copy neutral LOH or homozygous deletions were not observed. All detected
193 chromosomal gains were duplications of a single chromosome. *Gsp*⁺ tumors contained limited amount of
194 aneuploidy, mostly gains of single chromosomes. An exception was a tumor ST4 with genetic instability (GI%)
195 22% (Table 1, Supplementary Fig. S1). In addition, two *Gsp*⁻ tumors (ST5 and ST6) were totally aneuploidy-
196 free. GI% did not correlate with clinical variables (Supplementary Table S2). The observed recurrent
197 aneuploidy indicates selective advantage during tumorigenesis rather than random copy number alteration
198 (permutation test $P < 10^{-4}$; Supplementary Fig. S2).

199 An unsupervised hierarchical clustering analysis of gene expression demonstrated that aneuploidy was the
200 major determinant of somatotropinoma subtypes. Tumors clustered according to the aneuploidy rate as follows
201 (Figure 1A; principal components analysis in Supplementary Fig. S3). Twelve *Gsp*⁻ tumors with aneuploidy,
202 from now on called CA (chromosome aneuploidy)-tumors, clustered together. Accordingly, chromosome
203 stable (CS)-tumors with limited amount or no aneuploidy (7 *Gsp*⁺ and 2 *Gsp*⁻) formed their own distinct group.
204 When comparing expressions between CA- and CS-tumors, 881 differentially expressed transcripts ($FDR <$
205 5%, $|FC| > 2$) were identified (Supplementary Table S3). Integration of expression and SCNA data revealed
206 that 69.8% of differentially expressed transcripts locate at chromosomes with recurrent aneuploidy (≥ 4 tumors
207 with shared aneuploidy) from which 81.6% positively correlate with the chromosomal copy number change.
208 To understand the biological relevance of differentially expressed genes in CA-somatotropinomas, pathway
209 analysis was performed. The top canonical pathway emerged from the tumor subtype-specific expression was

210 the PKA pathway (Figure 1B, Supplementary Table S4). In this cAMP-mediated signaling pathway a majority
211 of molecules were upregulated in CS-tumor group indicating activated PKA signaling (Figure 2, Table 2). The
212 major inhibitors of cAMP levels [19], phosphodiesterases (PDEs) were up-regulated in CS-tumor group and
213 seven protein tyrosine phosphatase (PTP) receptors were differentially expressed between tumor groups (Table
214 2).

215 The expression pathway analysis also highlighted several pathways associated with cell cycle regulation and
216 explicitly in the *retinoblastoma 1/E2F transcription factor (RB1/E2F)* - mediated G1/S-checkpoint transition.
217 Among the enriched pathways were Molecular Mechanisms of Cancer, Chronic Myeloid Leukemia, Glioma,
218 Glioblastoma Multiforme, and Cell Cycle: G1/S Checkpoint Regulation (Figure 1B, Supplementary Table S4).
219 The genes showing expression differences between tumor groups accumulated in the RB1/E2F -mediated cell
220 cycle regulation and the subsequent G1/S-checkpoint transition indicating difference in mitotic progression
221 (Figure 1C.). *E2F4* transcription factor, a regulator of cell cycle [20], was downregulated in CA-tumor group.
222 By contrast, *histone deacetylase 5 (HDAC5)* and *RB transcriptional corepressor like 1 (RBL1/p107)*, both
223 repressors of E2F family members, were upregulated in CA-tumor group when compared to CS-tumors. Also
224 the anti-mitogenic growth factor *TGFβ2/SMAD3* signaling was downregulated in CA-tumor group (Figure
225 1C, Table 3).

226 Immunohistochemistry

227 Because RB1 is the major component of the complex regulating G1/S phase transition, protein levels of total-
228 and phosphorylated-RB1 were semiquantitatively assessed in tumors using immunohistochemistry. In all
229 tumors >90% of nuclei showed positive total- and phospho-RB1 staining. Because fractions of stained cells
230 were comparable between tumor groups, staining intensities were compared. Both tumor groups showed weak
231 to moderate nuclear immunoreactivity of total-RB1 (CA vs CS, 1.67 vs 1.78, $p = 0.6$, Student's t-test). In
232 addition, some occasional cytoplasmic total-RB1 staining was detected in both tumor groups. Phospho-RB1
233 showed weak to moderate nuclear staining in both tumor groups (1.59 vs 1.67, $p = 0.71$) (Supplementary Table
234 5, Supplementary Fig. S4).

235 To test PKA pathway analysis findings (Figure 2) at the protein levels, PTPRD and PTPRK IHCs were
236 performed. Tumor material was available from four CA- (ST10, ST12, ST18, ST19) and three CS-tumors

237 (ST15, ST17, ST21). In immunopositive tumors both PTPRD and PTPRK localized mainly in cytoplasm and
238 >90% of cells gave positive staining. PTPRD showed negative immunostaining in CA-tumors (*Gsp*⁻) and
239 moderate immunoreactivity in CS-adenomas (*Gsp*⁺). PTPRK immunostaining was negative or weak in CA-
240 tumors and moderate in CS-tumors (Supplementary Fig. 5).

241 To investigate the role of PTTG1 in the formation of aneuploidy, PTTG1 and Ki-67 immunostainings were
242 performed. Ki-67 and PTTG1 stainings were detected in all tumors. Ki-67 gave nuclear immunostaining.
243 PTTG1 immunopositive cells showed both nuclear and cytoplasmic localization. Most of the cells showed
244 predominant cytoplasmic localization, although there were also cells with predominant nuclear staining in both
245 tumor groups (Supplementary Fig. S6). All stained cells were scored and number of immunopositive cells were
246 significantly more abundant in CA-tumors compared to CS-adenomas ($\bar{x} = 1.8 \pm 1$ vs. 0.9 ± 0.5 , $P = 0.016$,
247 Wilcoxon-Mann-Whitney) (Table 1). The *PTTG1* RNA expression levels, emerging mainly from non-
248 proliferating cells, were comparable between CA- and CS-tumor groups (FC 1.05, $p = 0.733$). There were no
249 significant difference in Ki-67 scores between tumor groups ($\bar{x} = 2.7 \pm 1.6$ vs. 1.7 ± 1.2 , $P = 0.27$) (Table 1), but
250 as seen earlier [8, 21] the PTTG1 protein levels correlated with Ki-67 scores ($r = 0.62$, $P = 0.002$, Pearson's
251 coefficient).

252 DNA methylation

253 We surveyed DNA methylation and differentially methylated regions (DMRs) in 21 somatotropinomas by
254 targeted bisulfite sequencing (Supplementary Table S6). An unsupervised clustering of 50 000 CpG regions
255 with the largest variance between tumors showed, that apart from ST7 and ST21, the tumors clustered
256 according to the *Gsp* mutation status (Figure 3A; principal components analysis in Supplementary Fig. S7).
257 The genome-wide distributions of CpG methylation levels for different genomic contexts revealed that
258 methylation levels of promoter regions were comparable across tumors (Figure 3A). The rest of the annotated
259 regions showed hypomethylation of *Gsp*⁺ tumors (see below for the supervised analysis of *Gsp*⁺ and *Gsp*⁻).
260 Eighteen percentage of the differentially expressed (CA- vs CS) transcripts (119/670 coding transcript clusters;
261 Supplementary Table S3) were correlated with DNA methylation.

262 DNA methylation patterns are maintained and regulated by DNA methyltransferases (DNMTs), including
263 DNMT1, DNMT3A and DNMT3B [22]. We examined tumor-specific associations of *DNMT* expressions and
264 median CpG methylation and found that CpG methylation rates correlated with the *DNMT1* expression

265 (Spearman's rank correlation 0.49, $p=0.025$) (Supplementary Fig. S8), while *DNMT3A* (0.02, $p=0.929$) and
 266 *3B* (0.24, $p=0.294$) did not show correlation.

267 DNA methylation associates also with replication timing [17]. Supplementary Fig. S9 shows an overview of
 268 CpG methylation at different quartiles of replication timing. Majority of the tumors displayed the expected
 269 hypomethylation of late replicating regions (Spearman $\rho < 0$ and $P < 0.019$; Supplementary Table S7). The
 270 *Gsp*⁻ tumors ST10, ST11, ST16, and ST20 had an outstanding, positive correlation to replication time
 271 (Spearman $\rho > 0$ and $P < 0.018$), which suggests methylation maintenance also at late replicating regions. No
 272 clinical associations were found to explain the methylation maintenance difference in these four tumors (Table
 273 1).

274 Because the *Gsp* mutation status was the major factor behind the DNA methylation rates and profiles across
 275 tumors, DMRs were determined between *Gsp*⁺ versus *Gsp*⁻ somatotropinomas. Altogether, we found 1 369
 276 DMRs out of which 1 339 (97.8%) were hypomethylated in *Gsp*⁺ tumors: see Supplementary Table S8 for a
 277 complete list of all 1 369 regions' genomic coordinates and annotation of nearby (-20Kbp upstream; 2Kbp
 278 downstream) genes (1560 gene annotations). The Supplementary Table S8 is sorted by the absolute value of
 279 the test statistic, where negative effect direction denotes hypomethylation among the *Gsp*⁺ tumors compared to
 280 the *Gsp*⁻ tumors. Both the outstanding number of DMRs and the enrichment of *Gsp*⁺ tumors towards
 281 hypomethylation can likely be attributed to the genome-wide CpG methylation characteristics between the
 282 tumor types (see the unsupervised analysis and Figure 3A). The DMRs did not enrich among the aneuploidy
 283 chromosomes; 51% of the DMRs reside at recurrent aneuploidy, while the expected proportion was 55% based
 284 on the distribution of the TBS regions.

285 In addition to the DMR analysis, we also examined the genome-wide methylation profiles between *Gsp*⁺ and
 286 *Gsp*⁻ tumors in different genomic contexts. Supplementary Fig. S10 displays the CpG methylation levels in
 287 the context of promoters, enhancers, CpG islands and CCCTC-binding factor (CTCF) sites. The only
 288 systematic difference between the *Gsp*⁺ and *Gsp*⁻ tumors at these genomic contexts was the overall
 289 hypomethylation in *Gsp*⁺ tumors.

290 To assess the DNA methylation-expression association, the CpG methylation data was integrated with matched
 291 transcriptomes by expression quantitative trait methylation (eQTM) analysis [23, 24]. Consistent with previous
 292 studies, these associations account for only a small fraction of the assayed CpG sites and expressed genes [24].

293 In a supervised comparison, the differentially methylated regions between *Gsp*⁺ and *Gsp*⁻ tumors resulted in
 294 a total of 400 DMR regions with significant (FDR < 0.05) expression to methylation eQTM_s pertaining 155
 295 genes (Supplementary Table S9; see the Supplementary Fig. S11 for an unsupervised analysis of eQTM_s).
 296 Altogether, 392 DMR regions (98%), were hypomethylated in *Gsp*⁺ tumors and from these 333 (84.9%)
 297 showed positive eQTM⁺ association (hypomethylated in *Gsp*⁺ together with gene underexpression in *Gsp*⁺).
 298 This enrichment can be attributed mostly to the tumor subtype-specific differences in CpG methylation
 299 characteristics at gene body regions (Figure 3A).
 300 To identify biological functions associated with the methylation difference between *Gsp*⁺ and *Gsp*⁻
 301 somatotropinomas, we performed pathway analysis from the eQTM gene list. The majority of emerged
 302 pathways (22/31) were associated with inhibitory G α protein (G α_i)– and/or voltage-gated calcium channel
 303 (CaCn) signaling (Figure 3B, Supplementary Table S10). Both G α_i and Ca²⁺ signaling are previously
 304 connected to pituitary neoplasia [25, 26]. The inhibitory *G protein subunit alpha I-2* (*GNAI2*; G α_{i-2}) and *G*
 305 *protein subunit beta 1* (*GNB1*, G β_1) were upregulated in *Gsp*⁺ tumors (Figure 3C, Table 4). The CaCn
 306 members, *calcium voltage-gated channel subunit alpha 1A* and *1E* (*CACNA1A* and *CACNA1E*) and *calcium*
 307 *voltage-gated channel auxiliary subunit gamma 2* (*CACNG2*), were downregulated via hypomethylation
 308 (Supplementary Table S8).

309 DISCUSSION

310 Pituitary tumors are slowly growing benign neoplasia with a low mitotic activity due to senescence. Somatic
 311 SNVs and SVs are rarely found in these tumors, indicating that also other mechanisms are driving
 312 tumorigenesis [7, 8, 9, 10, 11, 12]. Aneuploidy is a common feature in solid tumors, and it provides cancer
 313 cells a mechanism to lose tumor suppressors and gain extra copies of oncogenes [13, 14]. However, a causal
 314 relationship between aneuploidy and tumorigenesis as well as genes/pathways that are deregulated by
 315 aneuploidy are still incompletely characterized [27]. Aneuploidy is a relatively common event in
 316 somatotropinomas [8, 12, 28]. In the current study, we were able to confirm that somatotropinomas create two
 317 subtypes associated with distinct aneuploidy rates and unique transcription profiles. The CA-tumor subtype
 318 contained *Gsp*⁻ tumors characterized by frequent and recurrent aneuploidy. Recurrent aneuploidy has been
 319 associated earlier with more malignant tumors [29], suggesting a selective advantage and role in the tumor

320 evolution in these cancer types. The other subtype, CS-tumors, contained all *Gsp*⁺ tumors together with two
321 *Gsp*⁻ adenomas. These tumors were either totally aneuploidy-free or displayed only single chromosome
322 number changes, indicating that expression changes caused by chromosome copy number alterations are
323 poorly tolerated in this tumor subtype.

324 In some tumor types, aneuploidy is associated with increased malignant potential, tumor recurrence, and drug
325 resistance [13, 14]. In the current study, clinical features of the patients (Supplementary Table S2) did not
326 associate with aneuploidy. Moreover, larger studies have shown that there is no difference in clinical
327 characteristics and outcome of the patients with or without *Gsp* mutation [6, 19], indicating that most aneuploid
328 *Gsp*⁻ tumors do not progress towards aggressive disease.

329 Because GH-secreting cells constitute only up to 45% of normal anterior pituitary cells [30] and because tumor
330 groups had their own expression signatures (Figure 1A), expression profile comparison was performed
331 between CA- and CS-tumor groups. Moreover, there was not normal anterior pituitary lobe tissue available for
332 the study. Differentially expressed genes in CA- and CS-tumors enriched most significantly in the PKA
333 signaling. It is well established that oncogenic *Gsp* mutations activate the cAMP-dependent PKA pathway [5].
334 Therefore this result reflects the *Gsp*⁺ tumor-induced activation of PKA signaling in the CS-tumor group. In
335 addition to the previously *Gsp*⁺ tumor - associated molecules, e.g. cAMP-specific PDEs [19], we found that
336 many protein tyrosine phosphatase (PTPs) receptors were differentially expressed in CA- and CS-tumor
337 groups. Moreover, PTPRD and PTPRK IHCs showed elevated protein levels in *Gsp*⁺ tumors. PTPs are known
338 to regulate crosstalk between cAMP and the mitogen-activated protein (MAP) kinase cascade [31], and
339 abundant enrichment of these genes imply the role for the PTP-signaling in the tumorigenesis of *Gsp*⁺
340 adenomas.

341 RB1/E2F complex has a major role in the cell cycle regulation. It controls the G1/S phase transition during the
342 cell cycle and is regulated by the RB1 pocket proteins (RB1, RBL1/p107, RBL2/p130) and E2F transcription
343 factors. Dysregulated G1/S-phase transition promotes tumor formation and may give rise to aneuploidy.
344 Inactivation of RB1 through phosphorylation leads release of E2F transcription factors and subsequent cell
345 cycle progression. RB1/E2F complex has shown to be involved in pituitary tumorigenesis. *Rb1* is a tumor
346 suppressor and mice with heterozygous inactivating *Rb1* mutation develop pituitary adenomas [20, 32, 33].
347 Our expression data showed that RB1/E2F-mediated G1/S –checkpoint signaling is differentially regulated

348 between the tumor groups. The CA-tumor group displayed downregulation of *E2F4*, whereas *E2F*-repressors
 349 *HDAC5* and *RBL1/p107* [34] were upregulated. *E2F4* is traditionally categorized as a transcriptional repressor,
 350 but more recently it was shown that in some tissue types *E2F4* may act as an activator of proliferation [35].
 351 The function of *E2F4* in GH-secreting pituitary cells is not elucidated. Interestingly, apart from *HDAC5*
 352 (17q21), all differentially expressed G1/S- related genes, *E2F4* (16q22), *RBL1* (20q11), and *TGF- β 2* (1q41),
 353 *SMAD3* (15q.22) locate on chromosomes with recurrent aneuploidy and their expression correlated with the
 354 direction of aneuploidy (Supplementary Fig. S1). We did not observed differences in protein levels of tot- and
 355 phospho-RB1 between CA- and CS-tumor groups. Immunohistochemistry is, however, a semiquantitative
 356 method and do not necessary detect more subtle protein level differences.

357 *The pituitary tumor-transforming 1 gene (PTTG1)* (5q33) is a mitotic checkpoint protein which regulates a
 358 sister chromatid segregation during mitosis as well as genes encoding G1/S and G2/M phase proteins [36, 37,
 359 38]. RNA and protein levels of PTTG1 exhibit a cell cycle–dependent expression pattern, being highest at
 360 G2/M phase and attenuated after mitosis. *PTTG1* is expressed in all types of pituitary tumors [39, 40]. Mice
 361 with overexpressed *Pttg1* develop pituitary adenomas, whereas knockout *Pttg1*^{-/-} animals do not [41, 42].
 362 Crossbreeding of overexpressed *Pttg1* animal with heterozygous *Rb1*^{+/-} mice increased penetrance of pituitary
 363 tumors. In contrast, crossbreeding of *Pttg1*^{-/-} animals with *Rb1*^{+/-} mice showed decreased tumor number and
 364 size, further supporting cooperative relationship between PTTG1 and RB1 in pituitary tumorigenesis [41, 42,
 365 43]. It has also shown that both loss and overexpression of *PTTG1* promote aneuploidy and G1/S cell cycle
 366 arrest induced senescence [43, 44, 45].

367 We showed that CA-tumors with recurrent aneuploidy exhibit higher PTTG1 protein levels. This finding
 368 together with the known function of PTTG1 in pituitary tumorigenesis [36, 39, 41, 43, 44] may indicate that
 369 elevated PTTG1 levels are involved in the development of aneuploidy in CA-somatotropinomas. During the
 370 initial steps of tumorigenesis, slowly accumulating aneuploidy can mediate excessive proliferation by
 371 changing gene expressions and modulating functions of pituitary tumor driver pathways. Eventually, however,
 372 recurrent aneuploidy leads to mitotic stress and senescence via altered levels of proteins involved in the
 373 RB1/E2F– mediated G1/S cell cycle progression. Thus, in CA-somatotropinomas aneuploidy may underlie
 374 both the tumor formation as well as escape from aggressive growth and malignancy.

375 Interestingly, *PTTG1* seems to be a downstream target of E2F transcription factor family [33]. However, the
376 regulatory mechanisms of *PTTG1* are only partially elucidated and further studies are required in order to
377 evaluate the role of PTTG1 in pituitary tumorigenesis.

378 Alterations of DNA methylation have been recognized as an important component of tumor development and
379 progression of cancer through different mechanisms. It has been shown, that pituitary tumors have their own
380 distinct DNA methylation profile without overlapping with other sellar region tumors [12]. The current work
381 shows that DNA methylation of somatotropinomas tends to cluster according to the *Gsp* mutation status. DNA
382 methylation levels can have longitudinal changes due to epigenetic reprogramming during tumorigenesis [46],
383 which may explain the observed mis-clustered tumors in our sample set. In general, *Gsp*⁺ tumors were
384 hypomethylated when compared to *Gsp*⁻ tumors and distributions of methylation levels for different genomic
385 contexts across tumors revealed distinct *Gsp* genotype-specific methylation profiles. DNMT1 is a
386 methyltransferase enzyme, which maintains DNA methylation during cell replication. Aberrant expression of
387 *DNMT1* is involved in tumor transformation and progression in many cancer types [22, 47]. In the present
388 study, expression of *DNMT1* was found to be positively correlated with tumor-specific methylation levels,
389 indicating involvement of *DNMT1* in the somatotropinoma tumorigenesis through establishment of
390 methylation levels.

391 *Gsp* genotype-specific DNA methylation profiles indicate that different molecular mechanisms are involved
392 in the development and progression of *Gsp*⁺ and *Gsp*⁻ pituitary tumors. The integration of DNA methylation
393 and gene expressions demonstrated that the inhibitory $G\alpha_i$ protein ($G\alpha_i$) signaling, together with the voltage-
394 gated calcium channel (CaCn) transducer signaling are the major biological functions differentially regulated
395 via DNA methylation in these tumor subtypes. In *Gsp*⁺ tumors $G\alpha_i$ signaling was activated through
396 overexpression of $G\alpha_{i-2}$ (*GNAI2*) and $G\beta 1$ (*GNBI*), whereas CaCn subunits were downregulated. Both of these
397 signaling cascades are involved in the regulation of cAMP response. Inhibitory $G\alpha_i$ proteins most notably
398 inhibit receptor-dependent cAMP synthesis [48]. CaCn signaling stimulates the cAMP response element-
399 binding (CREB) protein, a main downstream target of mitogenic effect of cAMP [26, 49, 50]. Thus, activated
400 $G\alpha_i$ and downregulated CaCn emphasize the adaptive response to elevated cAMP levels caused by *GNAS* ($G\alpha_s$)
401 mutation and hereby likely prevents the excessive cellular proliferation in *Gsp*⁺ tumors. We have earlier shown
402 that dysfunctional $G\alpha_i$ signaling and particularly the reduced $G\alpha_{i-2}$ protein levels contribute to the development

403 of *AIP* germline mutation associated somatotropinomas [25]. This study, however, shows for the first time the
404 essential role of $G\alpha_i$ signaling in *Gsp*⁺ somatotropinomas with constitutively activated cAMP synthesis.

405 The systematic characterization of the somatic landscape using genomic, epigenomic, and transcriptomic data
406 across *Gsp*⁺ and *Gsp*⁻ somatotropinomas highlighted tumor subtypes and subtype-specific mechanisms of
407 tumorigenesis. The study suggest association between increased PTTG1 protein levels and aneuploidy in *Gsp*⁻
408 adenomas, whereas *Gsp*⁺ tumors are characterized by DNA methylation controlled $G\alpha_i$ – CaCn signaling, a
409 response to the mitogenic cAMP-signaling caused by *GNAS* mutation. While further studies are needed to fully
410 characterize the molecular mechanisms resulting from aneuploidy-induced pituitary tumorigenesis, the work
411 presented here provides valuable new information about subtype-specific pituitary tumorigenesis. Moreover,
412 these findings may help to elucidate the mechanisms of aneuploidy also in other tumor types.

413 **Authors' Contributions**

414 Conception and design: N. Välimäki, A. Karhu

415 Development of methodology: N. Välimäki

416 Acquisition of data (provided animals, acquired and managed patients, provided facilities, etc.): C. Schalin-
417 Jäntti, A. Karppinen, L. Kivipelto, L.A. Aaltonen

418 Analysis and interpretation of data (e.g., statistical analysis, biostatistics, computational analysis): N.
419 Välimäki, A. Paetau, A. Karhu

420 Writing, review, and/or revision of the manuscript: N. Välimäki, C. Schalin-Jäntti, A. Karppinen, L. Kivipelto,
421 L.A. Aaltonen, A. Karhu

422 Administrative, technical, or material support (i.e., reporting or organizing data, constructing databases): N.
423 Välimäki, C. Schalin-Jäntti, L.A. Aaltonen, A. Karhu

424 Study supervision: A. Karhu

425 **Acknowledgements**

426 We thank Heikki Metsola, Sini Marttinen, Alison Ollikainen, Marjo Rajalaakso, Inga-Lill Åberg and Iina
427 Vuoristo for technical assistance. We acknowledge the computational resources provided by the ELIXIR node
428 hosted at CSC - IT Center for Science, Finland. The Biomedicum Imaging Unit (BIU) for the microscopy
429 service and Biomedicum Functional Genomics Unit (FuGU) for the microarray services are acknowledged.

430 **References**

- 431 1. Daly AF, Rixhon M, Adam C, Dempegioti A, Tichomirowa MA, Beckers A. High prevalence of
432 pituitary adenomas: a cross-sectional study in the province of Liege, Belgium. *J Clin Endocrinol Metab*
433 2006;91:4769-75.
- 434 2. Dekkers OM, Biermasz NR, Pereira AM, Romijn JA, Vandenbroucke JP. Mortality in acromegaly: a
435 metaanalysis. *J Clin Endocr Metab* 2008;93:9361–67.
- 436 3. Melmed S. Acromegaly pathogenesis and treatment. *J Clin Invest* 2009;119:3189–202.
- 437 4. Ritvonen E, Löyttyniemi E, Jaatinen P, Ebeling T, Moilanen L, Nuutila P, *et al.* Mortality in
438 acromegaly: a 20-year follow-up study. *Endocr Relat Cancer* 2016;23:469-80.
- 439 5. Vallar L, Spada A, Giannattasio G. Altered Gs and adenylate cyclase activity in human GH-secreting
440 pituitary adenomas. *Nature* 1987;330:566-8.
- 441 6. Ritvonen E, Pitkanen E, Karppinen A, Vehkavaara S, Demir H, Paetau A, *et al.* Impact of AIP and
442 inhibitory G protein alpha 2 proteins on clinical features of sporadic GH-secreting pituitary adenomas.
443 *Eur J Endoc* 2017;176: 243-52.
- 444 7. Newey PJ, Nesbit MA, Rimmer AJ, Head RA, Gorvin CM, Attar M, *et al.* Whole-exome sequencing
445 studies of nonfunctioning pituitary adenomas. *J Clin Endocrinol Metab* 2013;98:E796-E800.
- 446 8. Välimäki N, Demir H, Pitkänen E, Kaasinen E, Karppinen A, Kivipelto L, *et al.* Whole-Genome
447 Sequencing of Growth Hormone (GH)-Secreting Pituitary Adenomas. *J Clin Endocrinol Metab*
448 2015;100:3918-27.
- 449 9. Lan X, Gao H, Wang F, Feng J, Bai J, Zhao P, *et al.* Whole-exome sequencing identifies variants in
450 invasive pituitary adenomas. *Oncology Lett* 2016;12:2319-28.
- 451 10. Song ZJ, Reitman ZJ, Ma ZY, Chen JH, Zhang QL, Shou XF, *et al.* The genome-wide mutational
452 landscape of pituitary adenomas. *Cell Res* 2016;26:1255-9.
- 453 11. Ronchi CL, Peverelli E, Herterich S, Weigand I, Mantovani G, Schwarzmayer T, *et al.* Landscape of
454 somatic mutations in sporadic GH-secreting pituitary adenomas..*Eur J Endocrinol* 2016;174:363-72.
- 455 12. Capper D, Jones DTW, Still M, Hovestadt V, Schrimpf D, Sturm D. *et al.* DNA methylation-based
456 classification of central nervous system tumours. *Nature* 2018;555:469-74.

13. Carter SL, Eklund AC, Kohane IS, Harris LN, Szallasi Z. A signature of chromosomal instability inferred from gene expression profiles predicts clinical outcome in multiple human cancers. *Nat Genet* 2006;38:1043–8.
14. Weaver BA, Cleveland DW. Does aneuploidy cause cancer? *Curr Opin Cell Biol* 2006;18:658-67.
15. Farrell WE. Epigenetics of pituitary tumours: an update. *Curr Opin Endocrinol Diabetes Obes* 2014;21:299–305.
16. Karolchik D, Hinrichs AS, Furey TS, Roskin KM, Sugnet CW, Haussler D. *et al.* The UCSC Table Browser data retrieval tool. *Nucleic Acids Res* 2004;32:D493–96.
17. Chen CL, Rappailles A, Duquenne L, Huvet M, Guilbaud G, Farinelli L. *et al.* Impact of replication timing on non-CpG and CpG substitution rates in mammalian genomes. *Genome Res* 2010;20:447-57.
18. Shabalín AA. Matrix eQTL: Ultra fast eQTL analysis via large matrix operations. *Bioinformatics* 2012;28:1353-58.
19. Peverelli E, Mantovani G, Lania AG, Spada A. cAMP in the pituitary: an old messenger for multiple signals. *J Mol Endocrinol* 2013;52:R67–R77.
20. Manning AL, Dyson NJ. RB: mitotic implications of a tumour suppressor. *Nat Rev Cancer* 2012;12:220– 6.
21. Filippella M, Galland F, Kujas M, Young J, Faggiano A, Lombardi G, *et al.* Pituitary tumour transforming gene (PTTG) expression correlates with the proliferative activity and recurrence status of pituitary adenomas: a clinical and immunohistochemical study. *Clin Endocrinol* 2006;65:563-43.
22. Robertson KD, Keyomarsi K, Gonzales FA, Velicescu M, Jones PA. "Differential mRNA expression of the human DNA methyltransferases (DNMTs) 1, 3a and 3b during the G(0)/G(1) to S phase transition in normal and tumor cells". *Nuc Acids Res* 2000; 28:2108–13.
23. Kulis M, Heath S, Bibikova M, Queiros AC, Navarro A, Clot G *et al.* Epigenomic analysis detects wide-spread gene-body DNA hypomethylation in chronic lymphocytic leukemia. *Nat Genet* 2012;44:1236-42.

24. Gutierrez-Arcelus M, Lappalainen T, Montgomery SB, Buil A, Ongen H, Yurovsky A, *et al.* Passive and active DNA methylation and the interplay with genetic variation in gene regulation. *eLife* 2013;2:e00523.
25. Tuominen I, Heliövaara E, Raitila A, Rautiainen M, Mehine M, Katainen R, *et al.* AIP inactivation leads to pituitary tumorigenesis through defective G α i-cAMP signaling. *Oncogene* 2015;34:1174-84.
26. Nussinovitch I. Ca²⁺ channels in anterior pituitary somatotrophs: A therapeutic perspective. *Endocrinol* 2018;159:4043–55.
27. Beroukhin R, Mermel CH, Porter D, Wei G, Raychaudhuri S, Donovan J, *et al.* The landscape of somatic copy-number alteration across human cancers. *Nature* 2010;463:899-905.
28. Salomon MP, Wang X, Marzese DM, Hsu SC, Nelson N, Zhang X, *et al.* The Epigenomic Landscape of Pituitary Adenomas Reveals Specific Alterations and Differentiates Among Acromegaly, Cushing's Disease and Endocrine-Inactive Subtypes. *Clin Cancer Res* 2018;24:4126-36.
29. Knouse KA, Davoli T, Elledge SJ, Amon A. Aneuploidy in cancer: Seq-ing answers to old questions. *Annu Rev Cancer Biol* 2017;1: 335-54.
30. Bonert VS, Melmed S. Growth Hormone. *The Pituitary (Fourth Edition)* 2017; 85-127.
31. Saxena M, Williams S, Taskén K. Mustelin T. Crosstalk between cAMP-dependent kinase and MAP kinase through a protein tyrosine phosphatase. *Nature Cell Biol* 1999;1:305–10.
32. Jacks T, Fazeli A, Schmitt EM, Bronson RT, Goodell MA, Weinberg RA. Effects of an Rb mutation in the mouse. *Nature* 1992; 359: 295–300.
33. Zhou C, Wawrowsky K, Bannykh S, Gutman S, Melmed S. E2F1 induces pituitary tumor transforming gene (PTTG1) expression in human pituitary tumors. *Mol Endocrinol* 2009;23:2000–12
34. Dyson, N. The regulation of E2F by pRB-family proteins. *Genes Develop* 1998;12:2245-62.
35. Crosby ME, Almasan A. Opposing roles of E2Fs in cell proliferation and death. *Cancer Biol Ther* 2004;3:1208-11.
36. Romero F, Multon M-C, Ramos-Morales F, Domínguez Á, Bernal JA, Pintor-Toro JA, *et al.* Human securin, hPTTG, is associated with Ku heterodimer, the regulatory subunit of the DNA-dependent protein kinase. *Nucleic Acids Res* 2001;29:1300–07.

37. Pascreau G, Arlot-Bonnemains Y, Prigent C. Phosphorylation of histone and histone-like proteins by aurora kinases during mitosis. *Prog Cell Cycle Res* 2003;5:369–74.
38. Tong Y, Tan Y, Zhou C, Melmed S. Pituitary tumor transforming gene interacts with Sp1 to modulate G1/S cell phase transition. *Oncogene* 2007;26:5596–605.
39. Uccella S, Tibiletti MG, Bernasconi B, Finzi G, Oldrini R, Capella C. Aneuploidy, centrosome alteration and securin overexpression as features of pituitary somatotroph and lactotroph adenomas. *Anal Quant Cytol Histol* 2005;27:241-52.
40. Vlotides G, Eigler T, Melmed S. Pituitary Tumor-Transforming Gene: Physiology and Implications for Tumorigenesis. *Endo Rev* 2007;28:165–186.
41. Abbud RA, Takumi I, Barker EM, Ren SG, Chen DY, Wawrowsky K *et al.* Early multipotential pituitary focal hyperplasia in the alpha-subunit of glycoprotein hormone-driven pituitary tumor-transforming gene transgenic mice. *Mol Endocrinol* 2005;19: 1383 –91.
42. Donangelo I, Gutman S, Horvath E, Kovacs K, Wawrowsky K, Mount M, *et al.* Pituitary tumor transforming gene overexpression facilitates pituitary tumor development. *Endocrinology* 2006;147:4781–91.
43. Chesnokova V, Zonis S, Rubinek T, Yu R, Ben-Shlomo A, Kovacs K, *et al.* Senescence mediates pituitary hypoplasia and restrains pituitary tumor growth. *Cancer Res* 2007;67:10564-72.
44. Yu R, Lu W, Chen J, McCabe CJ, Melmed, S. Overexpressed pituitary tumor-transforming gene causes aneuploidy in live human cells. *Endocrinology* 2003;144:4991–8.
45. Kim D, Pemberton H, Stratford AL, Buelaert K, Watkinson JC, Lopes V, *et al.* Pituitary tumour transforming gene (PTTG) induces genetic instability in thyroid cells. *Oncogene* 2005;24:4861–6.
46. Doi A, Park IH, Wen B, Murakami P, Aryee MJ, Irizarry R, *et al.* Differential methylation of tissue- and cancer-specific CpG island shores distinguishes human induced pluripotent stem cells, embryonic stem cells and fibroblasts". *Nat Genet* 2009;41:1350–53.
47. Feinberg AP, Koldobskiy MA, Gondor A. Epigenetic modulators, modifiers and mediators in cancer aetiology and progression. *Nat Rev Genet* 2016;17:284–99.

- 536 48. Nürnberg B, Gudermann T, Schultz G. Receptors and G proteins as primary components of
537 transmembrane signal transduction. Part 2. G proteins: structure and function. J Mol Med
538 1995;73:123–32.
- 539 49. Bertherat J, Chanson P, Montminy M. The cyclic adenosine 3',5'-monophosphate-responsive factor
540 CREB is constitutively activated in human somatotroph adenomas. Mol Endocrinol 1995;9:777-83.
- 541 50. Shaywitz, AJ, Greenberg ME. "CREB: A Stimulus-Induced Transcription Factor Activated by A
542 Diverse Array of Extracellular Signals". Ann Rev Biochem 1999;68:821–61

543 **Authors' contributions**

544 **NV** processed, analyzed, and consolidated the data, provided statistical analyses, and contributed to the writing
545 of the manuscript. **CS-J** supported in the blood and tumor sample collections, provided the clinical and
546 laboratory parameters as well as the different treatments given to the patients, interpreted the clinical data, and
547 contributed to the writing of the manuscript. **LK** and **AtK** contributed to the blood and the tumor sample
548 collections for the study, and work with the manuscript preparation. **AP** provided pathological reviews for the
549 study. **LAA** provided support for the data collection, aided in interpreting the results, and worked on the
550 manuscript. **AK** analyzed and interpreted the data, provided statistical analysis, and contributed to the writing
551 of the manuscript. All authors read and approved the manuscript.

552

553 **SUPPLEMENTARY DATA:**

554 **Supplementary Methods** – Supplementary text containing details about mutation status validation of
555 established pituitary adenoma predisposing genes and IHC scoring.

556 **Supplementary Tables** - Supplementary Tables S1-S10 shows: 1) All the coding region variants (missense,
557 premature stop codon, frameshift) of 21 sequenced somatotropinomas that passed the somatic filtering. 2)
558 Results of correlation tests between genetic instability (GI%) and clinical variables. 3) Differentially expressed
559 transcripts ($FDR \leq 5\%$, $FC -2 \geq x \geq 2$) in CA- and CS-tumors. 4) Significantly enriched canonical pathways
560 carried out from differentially expressed genes ($FDR < 5\%$ and $|FC| > 2$; CA- vs CS-tumors). 5)
561 Immunostaining intensities of total- and phosphorylated-RB1 in CA- and CS-tumors. 6) CpG quality statistics.
562 7) Replication timing and CpG methylation. 8) Differentially methylated regions (DMRs) between *Gsp+*
563 versus *Gsp-* tumors, and nearby genes. 9) Integration of DMRs with matched transcriptomes by expression
564 quantitative trait methylation (eQTM) analysis (at 5% FDR). 10) The complete list of significantly ($p < 0.05$)
565 enriched cis-eQTM pathways.

566 **Supplementary Figures** - Supplementary Figures S1-9 show 1) Overview of the somatic copy-number
567 aberrations. 2) Enrichment of whole-chromosome deletions and amplifications. 3) Principal component
568 analysis of expression array data. 4) Total (tot) and phosphorylated (p) RB1 immunohistochemistry in CA-
569 and CS-tumors. 5) PTPR and PTPRK immunohistochemistry in CA- and CS-tumors. 6) Ki-67- and PTTG1

570 immunostainings. 7) Principal component analysis of CpG methylation estimates. 8) *DNMT1* and genome-
571 wide methylation. 9) Replication timing and CpG methylation. 10) Context-specific characteristics of CpG
572 methylation estimates. 11) Unsupervised analysis of expression quantitative trait methylation (eQTM).

Table 1. Characteristics of the patients. IGF-1 and PRL levels at diagnosis were compared to age- and sex-matched upper normal limits

Patient	Age at diagnosis /Gender	Elevated pituitary hormone	IGF-1 (% of UNL)	PRL (% of UNL)	Tumor size	Gsp status	No of surgeries	Radiotherapy	Current medical therapy	GI (%)	Ki-67 (%±SD)	PTTG1 (%±SD)
ST2 ^a	43/M	GH	329		macro	R201C	1	no	NA	4.9	0.9±0.17	0.5±0.21
ST3 ^a	37/M	GH/PRL	458	1340	macro	R201C	2	yes	yes	0	3.8±0.44	0.6±0.19
ST4 ^a	69/F	GH	207		micro	R201C	1	no	no	22	1.7±0.4	0.5±0.39
ST5 ^a	56/M	GH	177		macro	-	1	no	no	0	2.4±0.7	1.1±0.32
ST6 ^a	40/M	GH	313		macro	-	1	yes	yes	0	1.9±0.35	0.9±0.12
ST7 ^a	40/F	GH	189		macro	-	2	yes	NA ^b	34.1	3.5±0.31	1.7±0.38
ST8 ^a	55/F	GH	187		macro	-	1	no	NA	34.1	1.2±0.44	0.9±0.40
ST9 ^a	38/F	GH	202		macro	-	1	no	no	41.5	3.4±0.77	0.9±0.24
ST10 ^a	14/M	GH	14		macro	-	1	no	no	41.5	6.4±0.71	3.1±0.44
ST11 ^a	24/F	GH	138		macro	-	2	yes	no	43.9	1.8±0.54	1±0.34
ST12 ^a	37/M	GH	305		macro	-	2	no	yes	58.5	0.5±0.46	0.3±0.13
ST13	40/M	GH	247		macro	-	1	no	yes	32.1	1.4±0.47	1.7±0.43
ST14	59/M	GH	NA		NA	R201C	1	no	NA	0	0.5±0.45	0.7±0.26
ST15	62/F	GH	374		macro	R201C	1	no	NA	5.1	1.4±0.48	0.6±0.31
ST16	59/M	GH	57		macro	-	1	no	yes	43.6	1.0±0.42	1.7±0.27
ST17	45/M	GH	38		macro	Q227L	1	no	yes	0	0.6±0.19	0.8±0.22
ST18	26/F	GH	78		macro	-	1	no	no	46.2	4.1±0.64	2.6±0.30
ST19	53/F	GH	177		macro	-	1	no	yes	10.3	2.7±0.35	3.7±0.40
ST20	44/M	GH	135		micro	-	1	no	no	46.2	3.1±0.30	2.6±0.52
ST21	34/M	GH	274		macro	Q227L	1	no	yes	2.6	2.8±0.44	2.1±0.49
ST22	37/M	GH	234		macro	-	1	no	no ^b	25.6	1.9±0.37	1.5±0.39

Abbreviation: M, male; F, female; GH, growth hormone; PRL, prolactin; IGF-1, insulin-like growth factor 1; % of UNL, percent increase compared to upper normal limit; Gsp status, mutation observed; GI, genetic instability; PTTG1, pituitary tumor transforming gene 1. ^aWGS and SCNA data of tumors published in Välimäki *et al.* [8]. NA, not available; ^bnon-compliant, not in remission

Table 2. Differentially expressed genes in the PKA Signaling pathway (CA- vs CS-tumors).

Symbol	Entrez Gene Name	FC	FDR	Type	Symbol in Pathway
AKAP13	A-kinase anchoring protein 13	-2.820	0.017	other	AKAP
CAMK2D	calcium/calmodulin dependent protein kinase II delta	2.210	0.038	kinase	CAMK2
EYA1	EYA transcriptional coactivator and phosphatase 1	-6.640	0.021	phosphatase	PTP
NFAT5	nuclear factor of activated T-cells 5	-2.060	0.005	transcription regulator	NFAT
PDE10A	phosphodiesterase 10A	-2.840	0.042	enzyme	PDE
PDE4D	phosphodiesterase 4D	-2.660	0.026	enzyme	PDE
PDE7B	phosphodiesterase 7B	-4.840	0.001	enzyme	PDE
PHKB	phosphorylase kinase regulatory subunit beta	-3.370	0.000	kinase	PHK
PLCL1	phospholipase C like 1 (inactive)	-4.660	0.002	enzyme	PLC
PRKCD	protein kinase C delta	3.310	0.035	kinase	PKC
PTPRD	protein tyrosine phosphatase, receptor type D	-22.200	0.003	phosphatase	PTP
PTPRE	protein tyrosine phosphatase, receptor type E	-2.690	0.033	phosphatase	PTP
PTPRG	protein tyrosine phosphatase, receptor type G	-6.560	0.002	phosphatase	PTP
PTPRH	protein tyrosine phosphatase, receptor type H	3.220	0.011	phosphatase	PTP
PTPRJ	protein tyrosine phosphatase, receptor type J	3.810	0.026	phosphatase	PTP
PTPRK	protein tyrosine phosphatase, receptor type K	-7.020	0.007	phosphatase	PTP
PTPRS	protein tyrosine phosphatase, receptor type S	3.100	0.047	phosphatase	PTP
RAP1A	RAP1A, member of RAS oncogene family	-2.000	0.013	enzyme	RAP1
RYR2	ryanodine receptor 2	-7.880	0.001	ion channel	RYR
SMAD3	SMAD family member 3	-8.770	0.011	transcription regulator	SMAD3
TCF4	transcription factor 4	-2.450	0.013	transcription regulator	TCF/LEF
TGFB2	transforming growth factor beta 2	-2.120	0.046	growth factor	TGF- β

FC: expression fold change; FDR: false discovery rate

Table 3. G1/S Checkpoint Regulation enriched genes from expression pathway analysis (CA- vs. CS-tumors).

Symbol	Entrez Gene	FC	FDR	Type	Symbol in Pathway
E2F4	E2F transcription factor 4	-2.230	0.030	transcription regulator	E2F
HDAC5	histone deacetylase 5	2.180	0.004	transcription regulator	HDAC
RBL1	RB transcriptional corepressor like 1	2.080	0.006	transcription regulator	RBL1 (p107)
RBBP8	RB binding protein 8, endonuclease	-4.06	0.004	enzyme	RBBP8
SMAD3	SMAD family member 3	-8.770	0.010	transcription regulator	SMAD3
TGF-β2	transforming growth factor-β2	-2.120	0.045	growth factor	TGF-β

FC: expression fold change; FDR: false discovery rate

Table 4. Differentially regulated genes in the CREB Signaling pathway (*Gsp*⁺ vs. *Gsp*⁻).

Symbol	Entrez Gene	eQTM β	FDR	Type	Symbol in Pathway
CACNA1A	calcium voltage-gated channel subunit	3.77	0.001	ion channel	CaCn
	alpha1 A				
CACNA1E	calcium voltage-gated channel subunit	1.73	0.019	ion channel	CaCn
	alpha1 E				
CACNG2	calcium voltage-gated channel auxiliary	5.25	0.001	ion channel	CaCn
	subunit gamma 2				
GNAI2	G protein subunit alpha i2	-1.17	0.016	ion channel	G α /G α i
GNB1	G protein subunit beta 1	-1.40	0.021	ion channel	G β

eQTM β : Expression quantitative trait methylation, a correlation between gene expression and methylation, FDR: false discovery rate

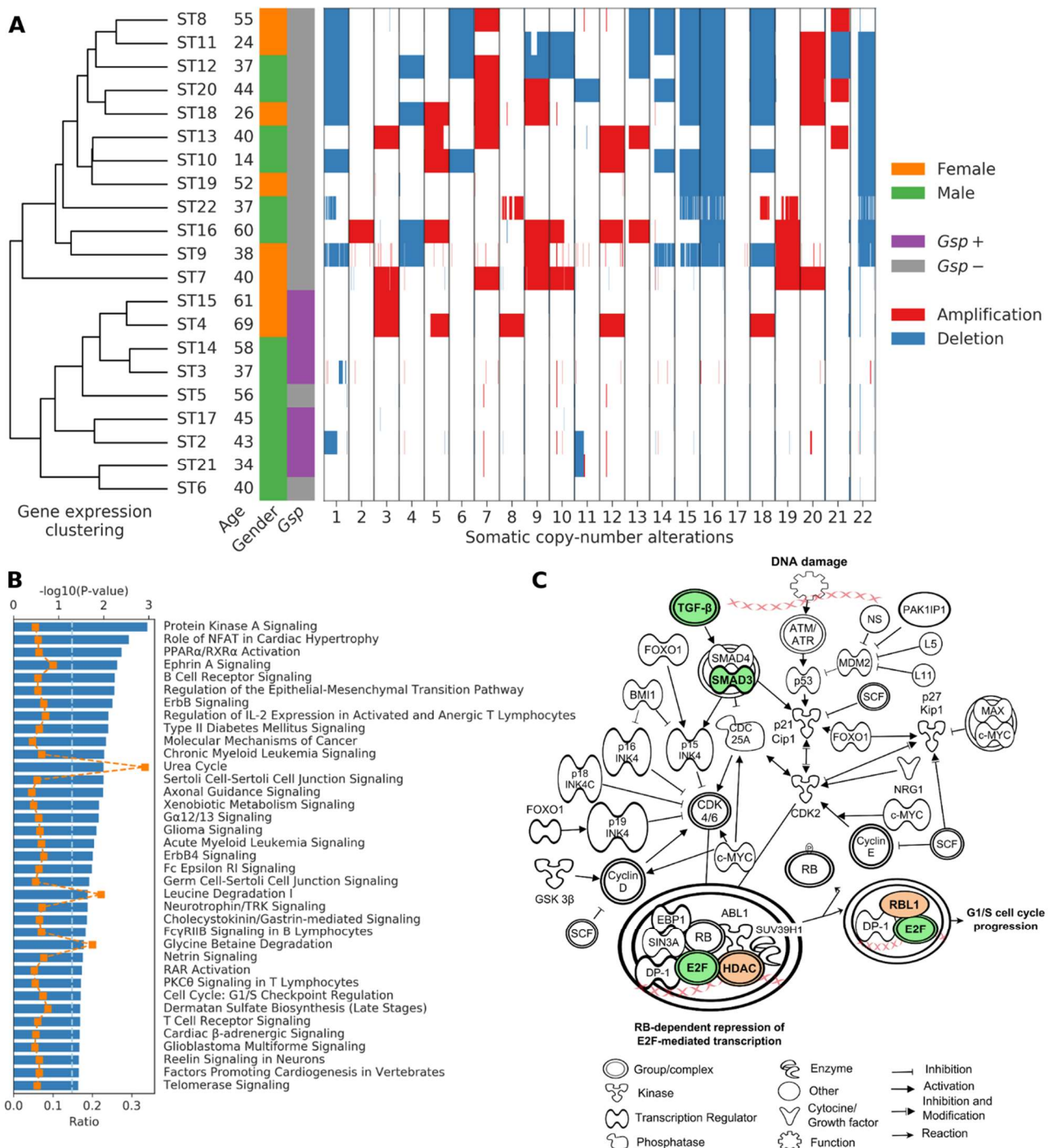
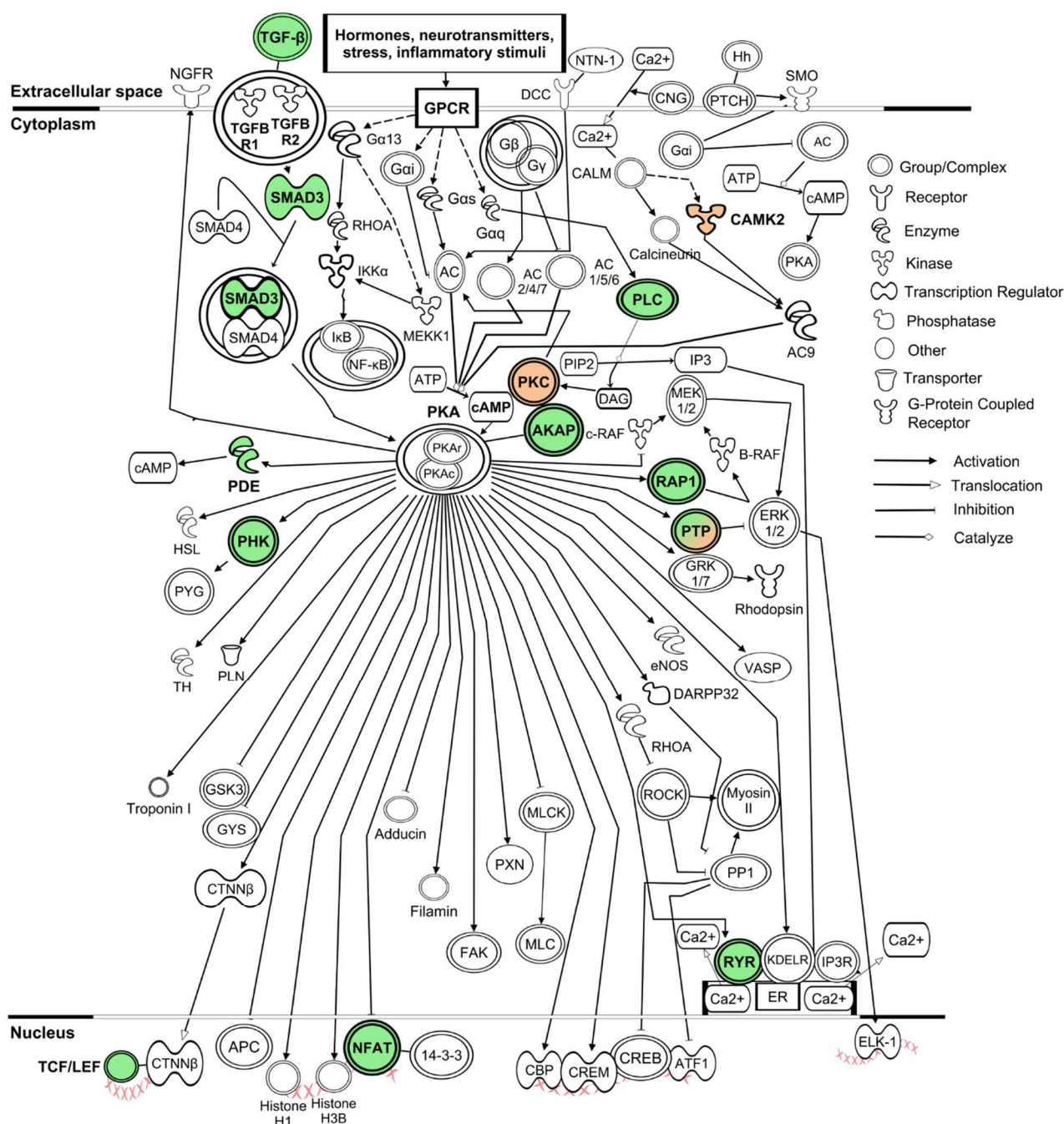


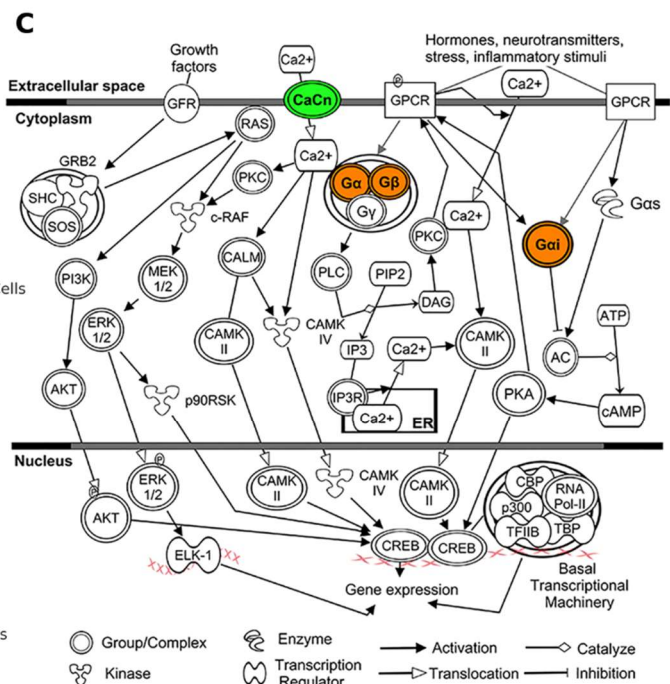
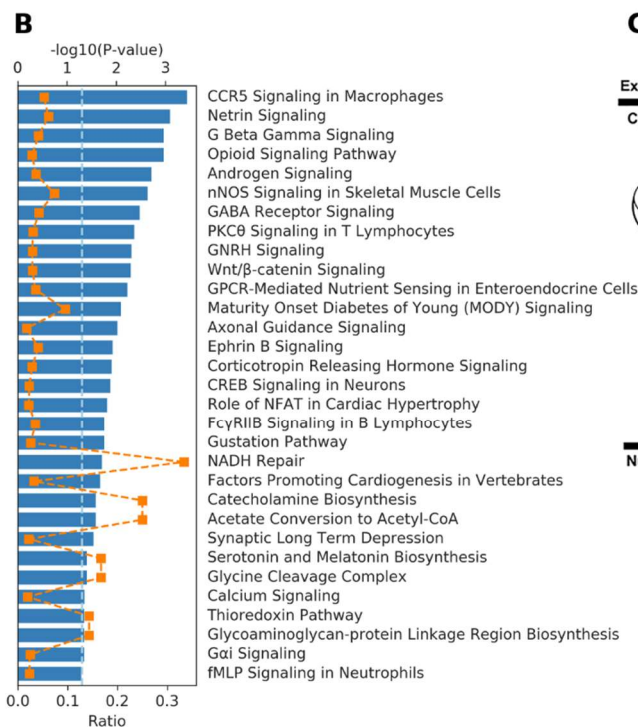
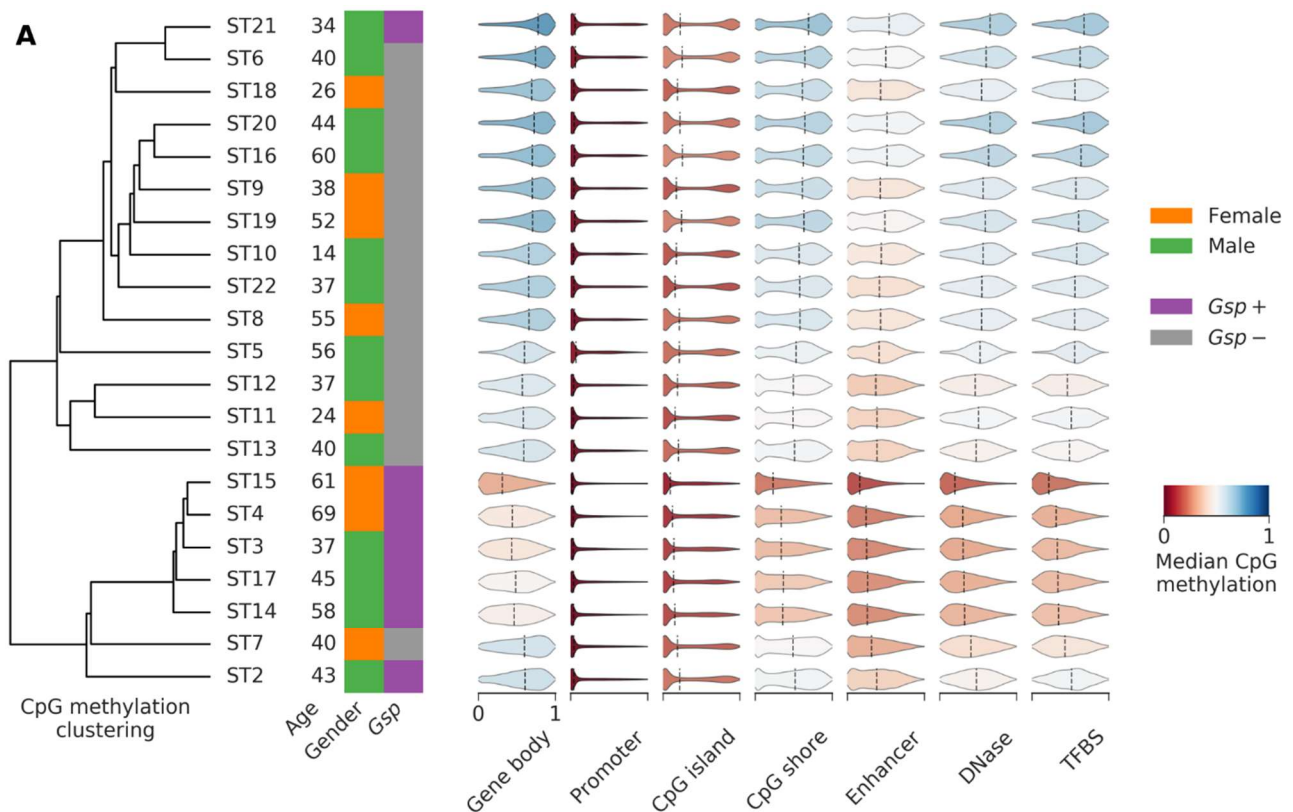
Figure 1. A, Gene expression of somatotropinomas clustered according to the aneuploidy rate. Left: Result of unsupervised hierarchical clustering of expression-array data from 21 somatotropinomas. Middle: Patients' age at diagnosis, gender, and *Gsp* mutation status. Right: Somatic copy-number aberrations. Supplementary: Fig. S1 shows all somatic chromosomal aberrations in more detail. Of note, the chr 1p of ST3 contains chromothripsis event [8]. **B**, Enriched pathways result from differentially expressed genes (CA- vs CS-tumors). Supplementary Table S4 shows the complete list of significantly ($p < 0.05$) enriched expression pathways and

589 genes. The blue horizontal bars denote the association P-values for each pathway on a logarithmic scale
590 (dashed vertical line at $p=0.05$). The ratio between the number of query genes found and total number of genes
591 in a pathway is shown in orange. C, The enriched G1/S Signaling pathway. The colored molecules identified
592 as differentially regulated in CA- vs CS-tumor groups. FCs and p-values are listed in Table 3. Orange label=up-
593 regulated; green label = down-regulated.



594

595 **Figure 2.** The enriched PKA Signaling pathway. The colored molecules identified as differentially expressed
 596 genes or gene groups in CA- vs CS-tumors. FCs and p-values are listed in Table 2. Orange label=up-regulated;
 597 green label = down-regulated.



598

599 **Figure 3. A**, CpG methylation of somatotropinomas clustered according to the *Gsp* mutation status. Left:
600 Unsupervised hierarchical clustering of CpG methylation data from 21 somatotropinoma samples (based on
601 50 000 regions with the largest variance between tumors). Middle: Patient's age at diagnosis, gender, and *Gsp*
602 mutation status. Right: Distribution of estimated CpG methylation levels for each genomic context: gene body

603 (from +2kb relative to the TSS to the end of gene), promoter (-1kb to +2kb relative to the TSS), CpG
604 island/shore, enhancer, DNase (DNaseI Hypersensitivity Cluster), and TFBS (Transcription factor cluster) (see
605 Materials and methods for details). Methylation levels are quantified by value ranging from zero
606 (unmethylated) to one (fully methylated). **B**, Pathway analyses from cis-eQTM. Supplementary Table S10
607 shows the list of significantly ($p < 0.05$) enriched cis-eQTM pathways and genes. The blue horizontal bars
608 denote the association P-values for each pathway on a logarithmic scale (dashed vertical line at $p=0.05$). The
609 ratio between the number of query genes found and total number of genes in a pathway is shown in orange. **C**,
610 The enriched CREB Signaling in Neurons pathway. The colored molecules identified as differentially
611 expressed *Gsp*⁺ vs *Gsp*⁻ tumors. eQTM- and FDR-values are listed in Table 4. Orange label=up-regulated;
612 green label = down-regulated.